

X-615-68-261

PREPRINT

NASA TM X-63285

# MEASUREMENTS IN THE IONOSPHERE OF THE ASPECT DEPENDENCE OF ANTENNA REACTANCE

## PART I: VARIATIONS ARISING FROM THE INHOMOGENEOUS PLASMA DISTRIBUTION ABOUT THE VEHICLE

ROBERT G. STONE  
JOSEPH FAINBERG  
J. K. ALEXANDER

JULY 1968



**GODDARD SPACE FLIGHT CENTER**  
**GREENBELT, MARYLAND**

**N 68-30003**

FACILITY FORM 502

(ACCESSION NUMBER)

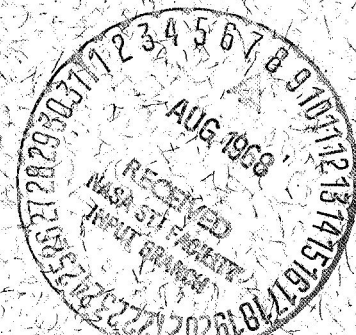
(THRU)

25  
(PAGES)

1  
(CODE)

TMX-63285  
(NASA CR OR TMX OR AD NUMBER)

07  
(CATEGORY)



MEASUREMENTS IN THE IONOSPHERE OF THE ASPECT

DEPENDENCE OF ANTENNA REACTANCE.

PART I:

VARIATIONS ARISING FROM THE INHOMOGENEOUS

PLASMA DISTRIBUTION ABOUT THE VEHICLE.

MEASUREMENTS IN THE IONOSPHERE OF THE ASPECT  
DEPENDENCE OF ANTENNA REACTANCE. PART I: VARIATIONS  
ARISING FROM THE INHOMOGENEOUS PLASMA DISTRIBUTION  
ABOUT THE VEHICLE

by

Robert G. Stone, Joseph Fainberg and J. K. Alexander

NASA-Goddard Space Flight Center  
Laboratory for Space Sciences  
Greenbelt, Maryland

ABSTRACT

Measurements of antenna reactance from a sounding rocket traveling through the ionosphere show variations related to the rocket spin period. The observed variations can be resolved into components with periodic time structure equal to the spin period, half the spin period, or a mixture of these. The relative importance of these components depends on the experiment configuration and the flight trajectory as well as on the magnetoionic parameters. To account for the observations, it is necessary to take into consideration the response of an antenna to the magnetoionic medium and to the disturbance produced in the ambient plasma by the rocket motion. Examples of the plasma distribution about the rocket, as inferred from the antenna reactance measurements, are shown and discussed.

## INTRODUCTION

Space observation of long wavelength radio emission as well as ionospheric plasma measurements by rf methods have, for the most part, utilized electrically short dipole antennas. When the antenna rotates as a result of spacecraft spin, the received signal as well as the measured driving point impedance vary with a periodicity related to the spin rate. The study of the causes of these effects is an interesting problem in radio physics and an essential subject for the proper interpretation of rf measurements. Spin dependent impedance variations have been reported by a number of investigators<sup>(1-3)</sup> although the sources of the variations have not been studied in any detail. In this series of papers consideration is given to two of the phenomena which contribute to the complex aspect dependence of antenna reactance.

Since the antenna is sensitive to the properties of the surrounding medium, there will generally be two ways in which the observed aspect dependence may arise. First, the terrestrial magnetic field renders the ionospheric plasma anisotropic so that the antenna characteristics depend on the angle between the antenna and the magnetic field. Secondly, there are a number of phenomena capable of producing an inhomogeneous plasma distribution in the vicinity of the antenna and spacecraft. For the present experiment, the major source of inhomogeneity is the disturbance produced in the plasma by the rocket motion at large velocities. This motion is capable of generating a downstream disturbance whose properties depend on rocket velocity and size, and on the characteristics of the medium. As the antenna aspect changes, impedance variations will be observed because the antenna samples the non-uniform plasma distribution about the rocket. The observed dependence of

antenna impedance on the magneto-ionic properties of the medium has been reported previously<sup>(2,4,5)</sup>. Emphasis here is entirely on the aspect variations.

The study of the disturbance produced about a body traveling through a plasma is of importance in many problems in space physics. Extensive theoretical analysis of this problem has been carried out for the "hyper-ionic" speed range where the body speed  $V_o$ , is much greater than the mean ion speed  $V_i$ , but much less than the mean electron speed  $V_e$ , i.e.,  $V_i \ll V_o \ll V_e$ . A general treatment of the theory is given in the comprehensive text by Alpert, Gurevich, and Pitalvskii<sup>(6)</sup>. At hyper-ionic speeds, the disturbance is expected to consist of a downstream wake depleted of ions and electrons and possibly a density compression ahead of the vehicle. The wake region extends downstream a distance of the order of  $R_o(V_o/V_i)$  where  $R_o$  is the characteristic size of the body. Within the central wake region, the average density departure from the ambient will be a function of  $(R_o/z)^2(V_o/V_i)^2$  where  $z$  is the distance from the body. Explicit expressions for the density and the range of validity may be found in the reference cited above. For example, the fractional deviation of the density in the wake  $n_2$  from its ambient value  $n_1$  is

$$\frac{\Delta n}{n} = \frac{n_2 - n_1}{n_1} = 1 - \frac{(z^2 - R_o^2)^{\frac{1}{2}}}{z} \exp - \left(\frac{V_o}{V_i}\right)^2 \left(\frac{R_o}{z}\right)^2 \quad (1)$$

valid for

$$z < R_o(V_o/V_i)^{\frac{1}{2}}$$

For many sounding rocket experiments, such as the one to be discussed here, the vehicle speed is more nearly "trans-ionic",  $V_0 \gtrsim V_i$ . Although the theory developed for  $V_0 \gg V_i$  cannot be expected to apply equally well here, some of the general characteristics of the disturbance should still be preserved. At these lower vehicle speeds, electric fields will play a more important role because they have a longer time to influence the motion of ions. It is partly for this reason that a theory valid in this speed range has not been developed.

Very few direct measurements of the disturbance about a space vehicle have been reported. The most recent of these observations may be found in the work of Henderson and Samir<sup>(7)</sup> which also contains a more complete reference to related theoretical and experimental work. But these direct measurements have been of the ion densities as derived from Langmuir probes. Radio frequency impedance measurements, on the other hand, will be sensitive to electron density variations.

Except for the strongly perturbed region near the vehicle, the electron density will follow the ion density variations because the difference between electron and ion densities decreases as  $(D/z)^2$ . The debye length  $D$ , for the altitude region of interest is of the order of a few millimeters. In addition to the normal ion sheath, an extended or "ram" sheath may exist in the region just behind the body. For the hyper-ionic limit where the difference of ion collection on the front and backside of the vehicle is large, the ram-sheath extends downstream a distance  $R_0$ . The electron density in this region is predicted to be very small since it is reduced from the ambient value by a factor of  $(D/R_0)^2$ . For  $V_0 \gtrsim V_i$ ,

the differential collection of ions will diminish as  $V_0$  decreases. In the limit of small  $V_0$ , the ram-sheath, if it exists, will become the normal ion sheath. For rf measurements made close to the vehicle, even a small ram-sheath should be observable.

Although the reactance variations arising from the plasma anisotropy will be considered in the second paper, a few comments are necessary here for the interpretation of the present measurements. For the plasma inhomogeneity arising from the vehicle induced disturbance, the angle  $\psi$  between the antenna and the rocket velocity vector will be most significant. For the plasma anisotropy, the angle  $\theta$  between the antenna and the magnetic field is of interest. The  $\theta$  dependence will enter through terms of the form (8,9)

$$C/C_0 \approx \alpha_1 \left( \cos^2 \theta + \frac{\alpha_3}{\alpha_1} \sin^2 \theta \right)^{\frac{1}{2}} \quad (2)$$

Where  $C/C_0$  is the ratio of antenna capacitance to its free space value. For a collisionless plasma

$$\alpha_1 = 1 - \frac{X}{1-Y^2}, \quad \alpha_3 = 1 - X, \quad X = \left( \frac{f_p}{f} \right)^2, \quad Y = \left( \frac{f_m}{f} \right)^2$$

and  $f_p$ ,  $f_m$ , and  $f$  are the electron plasma, electron gyro, and observing frequencies respectively. The strength of the anisotropy depends on  $\alpha_1/\alpha_3$ . For the analysis presented in this paper, observing conditions were selected to minimize the anisotropy, i.e., for  $\alpha_1/\alpha_3 \sim 1$ , so that this effect could be neglected.

## EXPERIMENTAL CONSIDERATIONS

The observations reported here were obtained from two separate experiments flown as part of Nike-Apache rocket payloads launched from Wallops Island, Va., on 16 July, 1964, at 1622 U.T. (dual monopole experiment) and 9 Sept. 1965, at 2358 U.T. (single dipole experiment). Both payloads attained an altitude in excess of 135 km.

The antenna system used for both experiments is shown graphically in Figure 1 to illustrate the relative size of the antenna elements, guard cylinder, and upper structure. The antenna is composed of two monopole elements which are extended after the release of a "clam shell" nose cone. Each monopole element was 45.5 cm. long and 1.26 cm. in diameter. A guard cylinder 15 cm. long, mounted coaxially at the base of each element, was maintained at the same rf potential as the rocket body. No dc bias was applied to the antenna elements. The antenna is employed as the capacitive element of an LC oscillator circuit. As the capacitance of the antenna changes, the frequency of the oscillator is counted digitally. From the known characteristics of the oscillator circuit and measurements of the free space oscillator frequency,  $f_0$ , the observed frequency  $f$ , in the ionosphere, can be converted into the corresponding value of  $C/C_0$ , the ratio of antenna capacitance in the medium to its free space value, where

$$C/C_0 = 1 + \frac{1}{4\pi^2 LC_0} \left( \frac{1}{f^2} - \frac{1}{f_0^2} \right) \quad (3)$$

$L$  and  $C_0$  are the oscillator inductance and antenna free space capacitance respectively. By writing the equation in this form, the base capacitance is eliminated. The system is able to measure relative changes of less than 1 percent in  $C/C_0$ .

For the single dipole experiment, the two monopole elements were connected as a conventional dipole and driven through a balun coil by the oscillator. For the dual monopole experiments, each monopole with its own associated oscillator system is electrically driven against the rocket body as shown in Figure 1. The two oscillator frequencies with corresponding free space values of 1.30 and 4.44 MHz, are read digitally at a rate of forty times per second. This provides a sampling rate which is large compared to the spin rate of approximately  $0.4 \text{ sec}^{-1}$ .

The monopole antenna system consists then of an asymmetric dipole composed of the short "monopole" element (45.5 cm) and the very long rocket body (475 cm). The rocket body radius  $R_0$  is 8.4 cm. Therefore, measured from the rocket axis, the monopole emerges from the guard cylinder at a distance  $z = 23.4 \text{ cm}$ . This distance will be considered as the "effective" sampling distance of the monopole. We are treating the antenna as if it were composed of a small sleeve monopole elevated above a ground plane (the rocket body). This is only a crude approximation since the entire antenna will be sensitive to the properties of the medium. Note in any case, however, that as the monopole element rotates it will be sensitive to azimuthal variations in the properties of the medium.

Since the magnitude as well as the direction of  $\bar{V}_0$  relative to the axis of the rocket body plays a very significant role in this experiment, the locus of  $\bar{V}_0$  for the trajectory is shown in Figure 2. In this figure the cross section of the rocket and the relative position of the antenna system is also shown.

## RESULTS

In Figure 3, a section of the spin modulation of monopole antenna reactance at 4.44 MHz is shown for observations near apogee. Except for small random deviations, which may indicate turbulence, the pattern is essentially sinusoidal. The modulation is produced as the antenna rotates through a region of varying properties. At this observing frequency, the minima of the curve correspond to the point of lowest electron density encountered by the antenna during its rotation.

From the trajectory information and the magnetometer aspect data, the direction corresponding to the reactance minima is found to be within  $\pm 5^\circ$  of the velocity direction ( $-\bar{V}_0$ ). Note that relative to  $\bar{H}$ , the magnetic field direction,  $\bar{V}_0$  and consequently the position of the reactance minima will shift continuously through the trajectory (see Figure 2). In the case of modulation arising from anisotropy, the reactance extremum will not shift relative to  $\bar{H}$ .

Note, furthermore, that the modulation observed, for example, in Figure 3 is more than an order of magnitude larger than that expected from the magneto-ionic effect. For a 4.44 MHz observing frequency,  $Y = 0.33$ , and  $0 \leq X \leq 0.2$  for this experiment. For  $X = 0.2$ , the anisotropy is greatest,  $\alpha_1/\alpha_3 \sim 0.969$ . For a Wallops Island launch,  $\theta$  will vary between  $68^\circ$  and  $90^\circ$ . According to Equation 2, the difference in reactance between the extreme values of  $\theta$  will be 0.003. But from Figure 3, the difference of reactance at the extremes is approximately 0.15, or 50 times larger than expected from the magneto-ionic effect.

When a dipole antenna is used, it will sample the wake region twice per rotation as each of its monopole elements passes through the wake. To confirm this, one spin period of data from the monopole and dipole experiments are compared in Figure 4. Since the two sets of data were obtained from separate flights, it was necessary for comparison to align them by using the appropriate aspect data, and to account for slightly different spin periods. Unless care is exercised in the analysis of dipole experiments, it is not possible to determine if the modulation results from the inhomogeneity or from the anisotropy. Since the anisotropy enters through  $\sin^2\theta$  and  $\cos^2\theta$  terms, it will also lead to variations at two cycles per spin period. For this reason it is necessary to know the flight geometry and trajectory as well as the properties of the medium.

Reactance data for the same range of ascent and descent trajectory are shown in Figure 5. The gradual change of reactance with altitude is caused by the electron density gradient in this ionosphere altitude range. The most striking difference between these curves is the more pronounced modulation during descent. At a specific altitude, the velocity magnitude for either ascent or descent is essentially the same. The difference between the curves must be associated with the direction of  $\bar{V}_0$ . This is indeed the case as may be seen by referring back to Figure 2. During ascent, only the small irregular rocket structure above the antenna produces the wake. For descent the entire lower rocket body causes the wake. Note also in this figure, how a change in the direction of  $\bar{V}_0$  causes a change in the extent of antenna within the wake. For descent, the

shadowing by the rocket body is effective enough to cause  $C_0/C$  to approach unity indicating very small electron densities in the wake region.

Except for small variations presumably caused by the irregular shadowing structure, the ascent data has only one minima; that corresponding to the wake direction. The descent data, however, shows a secondary smaller minimum or wake located at a position corresponding to the front of the vehicle. This secondary wake occurs only during descent and was eventually traced to the presence of another antenna system located further down on the rocket body. This small wake shall be neglected in the analysis to follow. The arrows in Figure 5 represent magnetometer markers. Note that the positions of corresponding markers is different for ascent and descent, and they do not correspond to reactance minima or maxima. In other words, the reactance is not "locked" to the magnetic field as would be the case for the plasma anisotropy.

### ANALYSIS

We have demonstrated that the observed reactance variations at this frequency are caused by the motion of the antenna through a non-uniform plasma distribution. In the following section, the observations will be used to infer the properties of this non-uniform distribution.

Since  $Y^2 \ll 1$ , and the anisotropy is small, Equation 2 may be approximated by

$$C/C_0 \sim [1 - (f_p/f)^2] \quad (4)$$

or

$$f_p = 9 n^{\frac{1}{2}} \text{ (kHz)} \approx (1 - C/C_0)^{\frac{1}{2}} f$$

Using this expression in Equation 3, leads to

$$\frac{\Delta n}{n_1} = \frac{n_1 - n_2}{n_1} = \frac{f_1^2 - f_2^2}{f_1^2 - f_0^2} \quad (5)$$

where  $n_1$ ,  $n_2$  are the electron densities corresponding to the measured frequencies  $f_1$ ,  $f_2$  respectively, and  $n_1$  is taken to be the ambient density. Note that the nature of  $\Delta n/n_1$  will depend on the choice for  $n_1$ . Initially we assume that the density measured when the antenna is in the direction of motion ahead of the vehicle corresponds to the unperturbed density. This choice will be reconsidered later.

The density in the wake\*at a fixed radial distance from the rocket is expected to be a function of the relative rocket speed. In Figure 6  $\Delta n/n_1$  is shown for  $1 \leq V_o/V_i \leq 2.4$  during the descent phase of the trajectory. The value of  $V_i$  is assumed to be 400 meters/sec and is based on a mean ion mass  $M = 28$  and  $T = 230^\circ\text{K}$  appropriate to an altitude of 100 km. The significance of Figure 6 must be considered carefully because of the large variation in the angle of attack as well as magnitude of the velocity  $V_o$  relative to the rocket body axis. Referring back to Figure 2, it is seen that for the apogee altitude region where  $(V_o/V_i) \sim 1$  the angle of attack is approximately perpendicular to the rocket body axis. However, during descent the angle of attack changes rapidly until it approaches  $50^\circ$  at the end of the observations. In essence this means that the cross sectional area producing the shadow as well as the position of the antenna in the wake will vary along with  $V_o/V_i$ . It is not clear how these parameters can be

taken into account properly with only limited data available. A systematic increase of  $\Delta n/n_1$  with  $V_o/V_i$  can be seen in Figure 6 as expected. The rocket coning and nutation motion results in a periodic oscillation of the plane of antenna rotation relative to the wake region. The dotted lines in Figure 6 represent the extremes of  $\Delta n/n_1$  as a result of this effect. The limits of variation decrease with increasing  $V_o/V_i$  because the angle of attack has now moved the antenna system well within the wake region so that the coning or nutation motion has less effect than near apogee where the motion can cause the antenna to cross the edge of the wake. The sensitivity of  $\Delta n/n_1$  to the angle of attack implies that perhaps a good part of the systematic change shown in Figure 6 is caused by the change of this angle. Therefore, in this figure the angle of attack is also shown. At larger velocities,  $V_o/V_i > 1.6$ , the angle of attack does not change rapidly and it is reasonable to assume that the observed change of  $\Delta n/n_1$  is now primarily a velocity effect.

The variation of  $\Delta n/n_1$  as a function of the angle  $\psi$  measured around the rocket from the direction  $V_o$  is shown in Figure 7 for a number of typical cases. In arriving at these curves, the value of  $n$  at  $\psi = 0$ , i.e., in front of the vehicle, was assumed to represent the ambient density  $n_1$ . For curve "A",  $V_o/V_i \approx 1$ , the disturbance is not very large and the density slowly approaches its assumed ambient value at  $\psi = 0$ . On the axis of the wake  $n = 0.62 n_1$ . For curve "B",  $V_o/V_i = 1.2$ , the general behavior is similar to "A" but the density approaches the assumed ambient value more rapidly and the density on the wake axis is smaller,  $n = 0.52 n_1$ . For curve "C",  $V_o/V_i = 2.14$ , the disturbance is beginning to decrease more rapidly towards the front of the vehicle; the density on

the wake axis is  $n = 0.31 n_1$ . Note that here and in the following case, the small secondary disturbance generated ahead of the vehicle has been neglected. For curve "D",  $V_o/V_i = 2.44$ , the density on the wake axis is  $n = 0.20 n_1$  but the disturbance appears as if it may have reached a maximum value not on the wake axis but at an angle of approximately  $\psi = 160^\circ$  or  $20^\circ$  from the wake axis. The effect is small; however, the difference in the disturbance at  $160^\circ$  and  $180^\circ$  amounts to  $\frac{1}{2}$  percent which is close to the experimental error. Nevertheless, this effect is observed for the larger values of  $V_o/V_i$  and might be an indication of the mach cone structure. For  $V_o/V_i = 2.44$ , this cone half angle is expected to be of the order of  $30^\circ$ . The existence of a density below the ambient value measured for  $\psi > 90^\circ$  may result from the antenna integration over a volume of space. When the antenna is at  $\psi > 90^\circ$  it may still be sensing contribution from regions corresponding to  $\psi < 90^\circ$ .

Most of the questions raised in connection with interpretation of the data shown in Figure 6 apply equally well here. However, given a specific set of conditions of the angle of attack and  $V_o/V_i$ , the curves in Figure 7 do accurately depict the relative variation of the density distribution about the rocket. But the form of this distribution will depend on the choice of the position selected for  $n_1$ . One may reasonably object to the position corresponding to  $\psi = 0$  for the ambient density because of a region of increased density or compression may exist there; The value of  $n_1$  at  $\psi = 90^\circ$  might be considered a better choice, particularly at larger values of  $V_o/V_i$ . The choice of a position of minimum disturbance will be a function of rocket velocity, although the concept of an unperturbed ambient density anywhere in the near

vicinity of the vehicle is at best an approximation.

For the purpose of comparison, the curves in Figure 7 have been replotted in Figure 8 for  $n_1$  at  $90^\circ$ . This "forces" the disturbance to zero at  $\psi = 90^\circ$  and leads to negative values of  $\Delta n/n_1$  for smaller angles. The negative values represent a density increase over the assumed ambient value. This choice for  $n_1$  also insures that the region of decreased density occurs behind the rocket, i.e. for  $\psi \geq 90^\circ$ .

### CONCLUSION

Measurements made from a sounding rocket traveling through the ionosphere show aspect dependent impedance variations. Several phenomena contribute to these variations. One source of variation is shown to arise from an inhomogeneous plasma distribution about the rocket. As the antenna rotates because of rocket spin, this non-uniform distribution is sampled continuously. It is possible to study this effect with negligible interference from plasma anisotropy by observing at an adequately high frequency.

The properties of this non-uniform distribution about the rocket have been inferred from the rocket impedance variations. A wake region of depleted electron density is found behind the body. The electron density in the wake depends on the relative rocket speed and direction. The wake structure at the antenna effective sampling radius is relatively smooth, although there is some indication of turbulent structure. The antenna is however, a volume integrating device, so that small scale turbulent structure would be difficult to observe. In deriving the normalized density distribution, uncertainty exists in how to choose a value for the ambient (undisturbed) density. Several alternatives are considered.

This new method of studying the disturbed density distribution about a space vehicle and the properties of the wake shows considerable promise. In any case, it is clear that this non-uniform plasma distribution must be considered in the interpretation of many rf measurements.

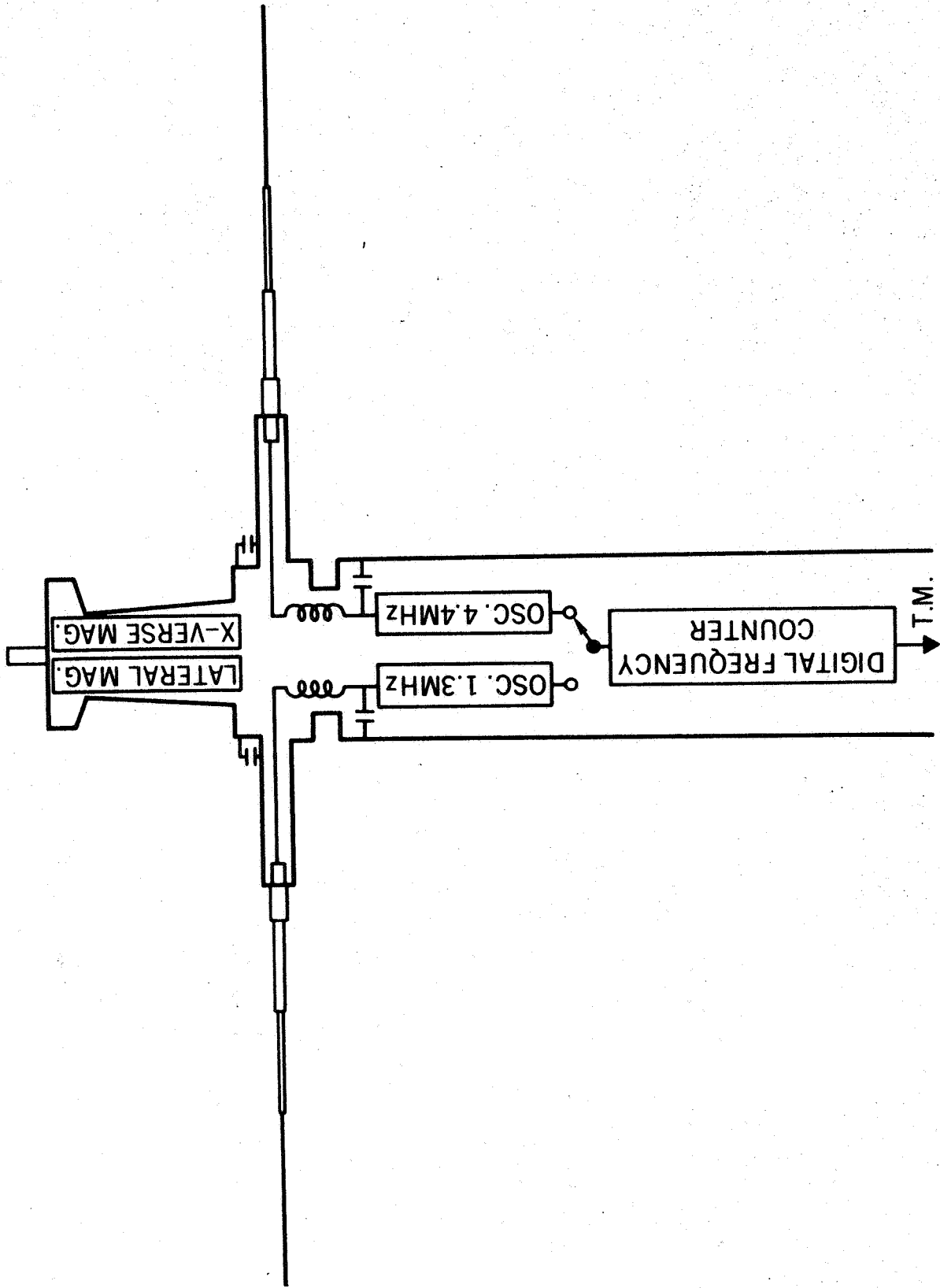
## CAPTIONS

- Figure 1. Experimental configuration for the dual monopole experiment. For the dipole experiment the oscillator was connected through a balun to the two monopole elements.
- Figure 2. Locus of rocket velocity  $\bar{V}_0$  relative to the rocket body axis during the flight trajectory on 16 July 1964.
- Figure 3. Spin modulation of normalized monopole antenna reactance at upper frequency (free space measurement frequency 4.44 MHz).
- Figure 4. Spin modulation of antenna reactance during comparable portions of the trajectories for the dipole experiment and for the monopole experiment.
- Figure 5. Spin modulation of normalized monopole antenna reactance for comparable portions of the descent and ascent trajectories (free space measurement frequency 4.44 MHz).
- Figure 6. Fractional electron density in wake during portion of descent trajectory.
- Figure 7. Fractional electron density over one half spin cycle. For curve A,  $V_0/V_i = 1$ ; curve B,  $V_0/V_i = 1.2$ ; curve C,  $V_0/V_i = 2.14$ ; curve D,  $V_0/V_i = 2.44$ .  $\Delta n$  taken as zero at  $\psi = 0$ .
- Figure 8. Fractional electron density over one half spin cycle. Curve labels same as Figure 7.  $\Delta n$  taken as zero  $\psi = 90^\circ$ .

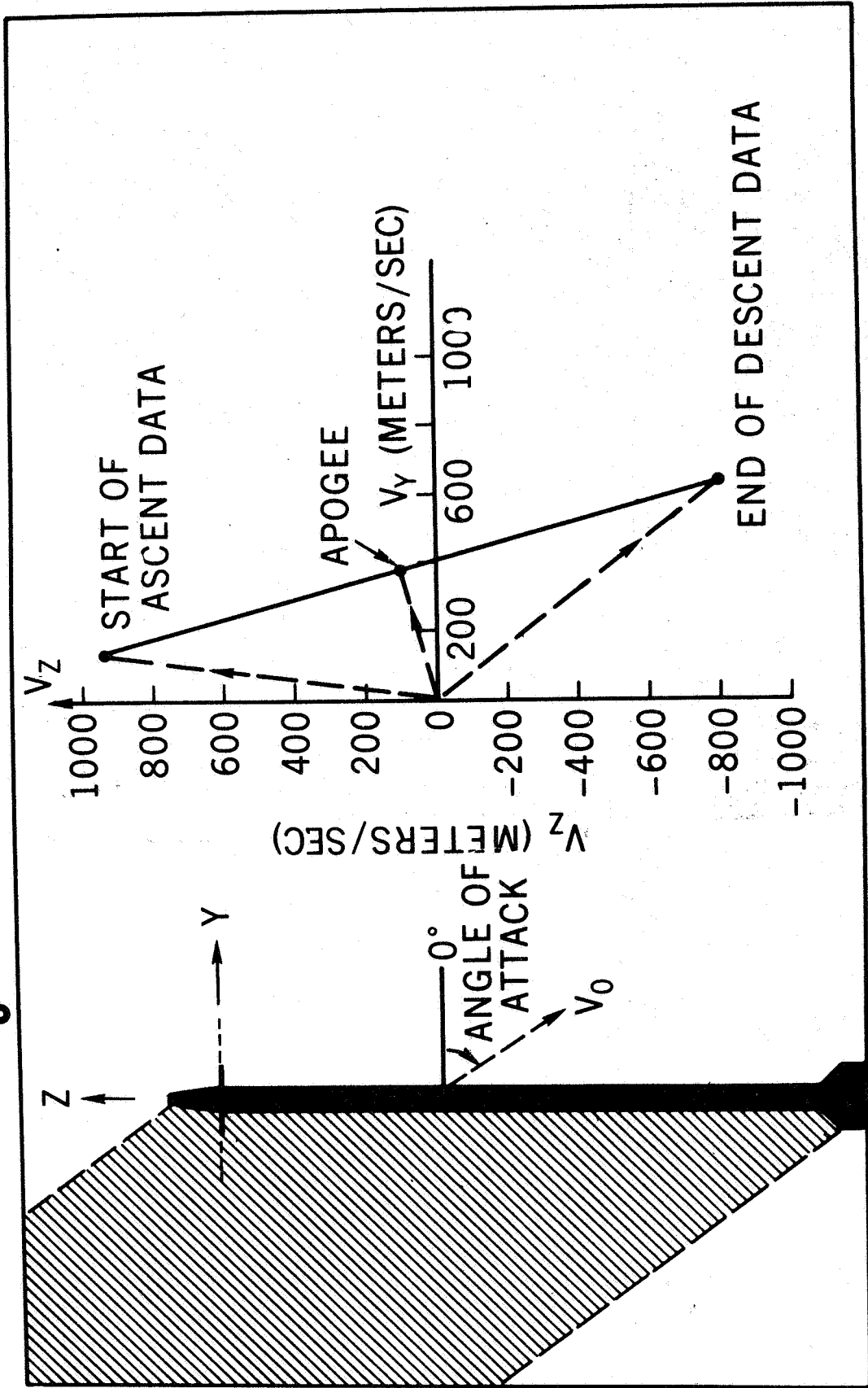
## REFERENCES

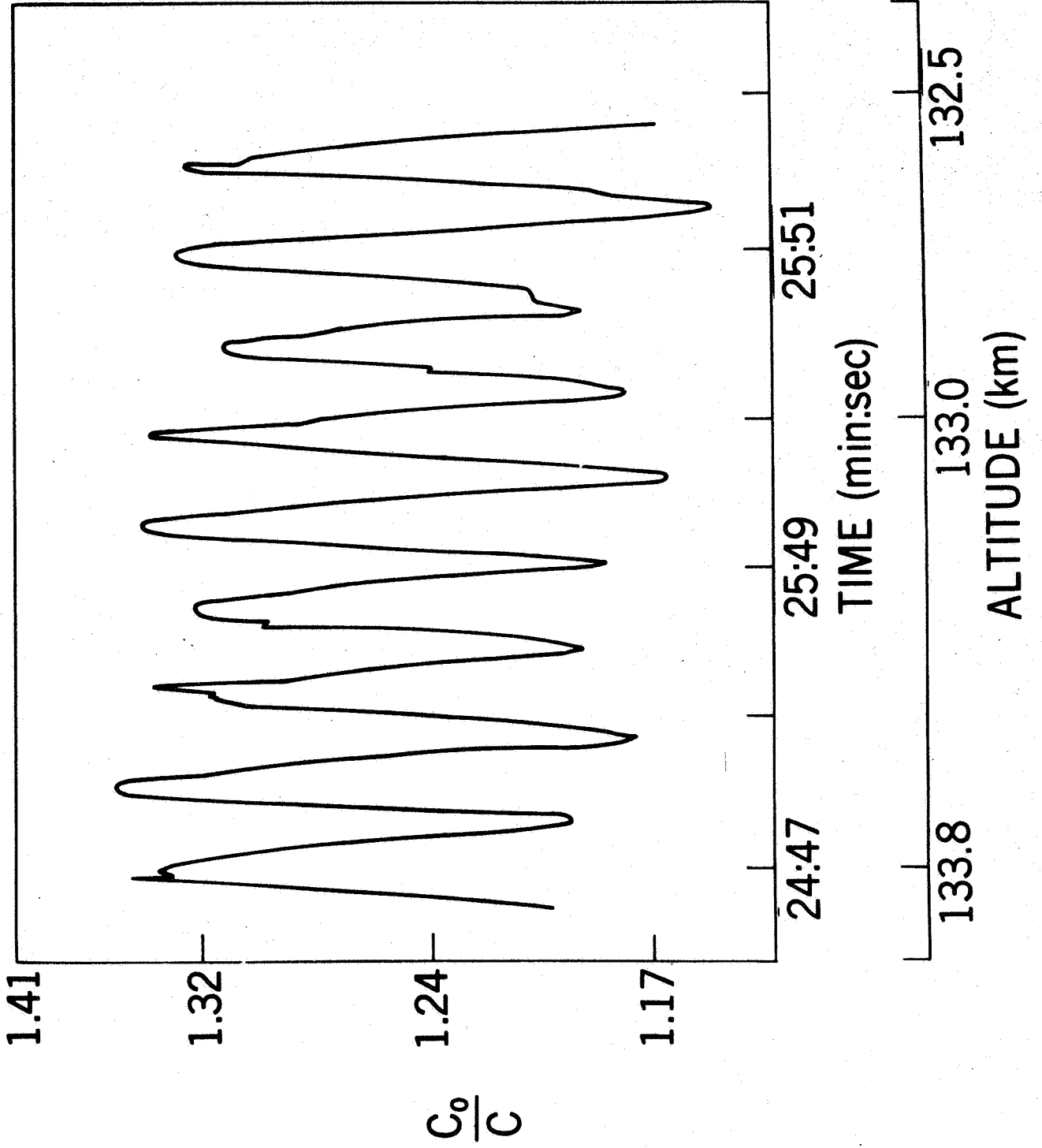
1. E. N. Bramley, "Planet. Space Sci.", 13, 979 (1965).
2. R. G. Stone, J. K. Alexander, R. R. Weber, "Planet. Space Sci.", 14, 1227 (1966).
3. O. Holt, G. M. LerFald, "Radio Science", 2, 1283 (1957).
4. R. G. Stone, R. R. Weber and J. K. Alexander, "Planet. Space Sci.", 14, 631 (1966).
5. R. G. Stone, J. K. Alexander and R. R. Weber, "Planet. Space Sci.", 14, 1007 (1966).
6. Al'pert, Gurevich, Pitaevskii, Space Physics with Artificial Satellites, Translated by H. H. Nickle, Consultants Bureau, New York, 1965.
7. C. L. Henderson, U. Samir, "Planet, Space Science" 15, 1499 (1967).
8. K. G. Balmain, IEEE "Trans. Antennas Propag.", 12, 605, (1964).
9. T. R. Kaiser, "Planet. Space Sci.", 9, 639, (1962).

# DUAL "MONOPOLE" ANTENNA EXPERIMENT.



# LOCUS OF $\vec{V}_0$ RELATIVE TO THE ROCKET BODY AXIS





DIPOLE EXPERIMENT

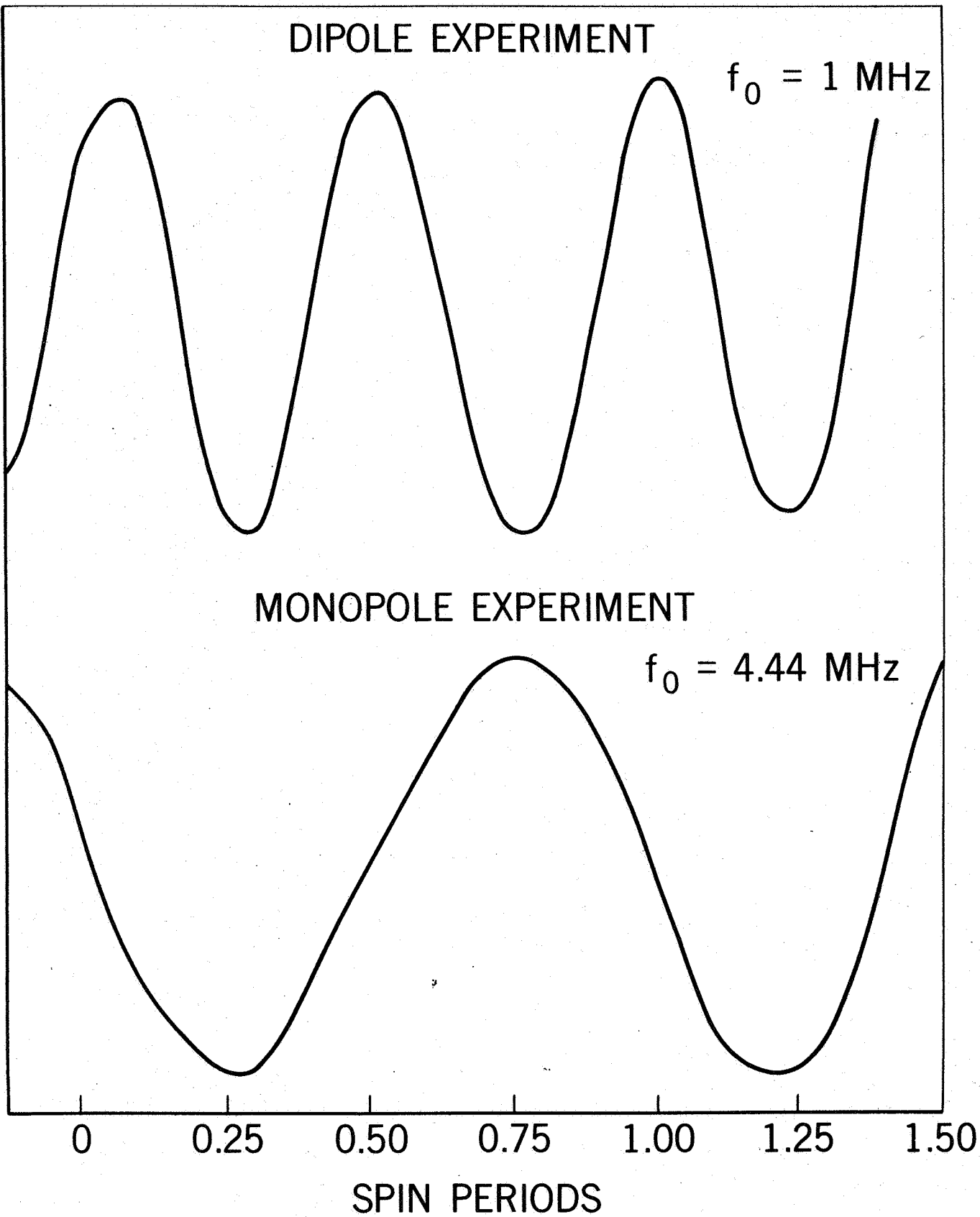
$f_0 = 1 \text{ MHz}$

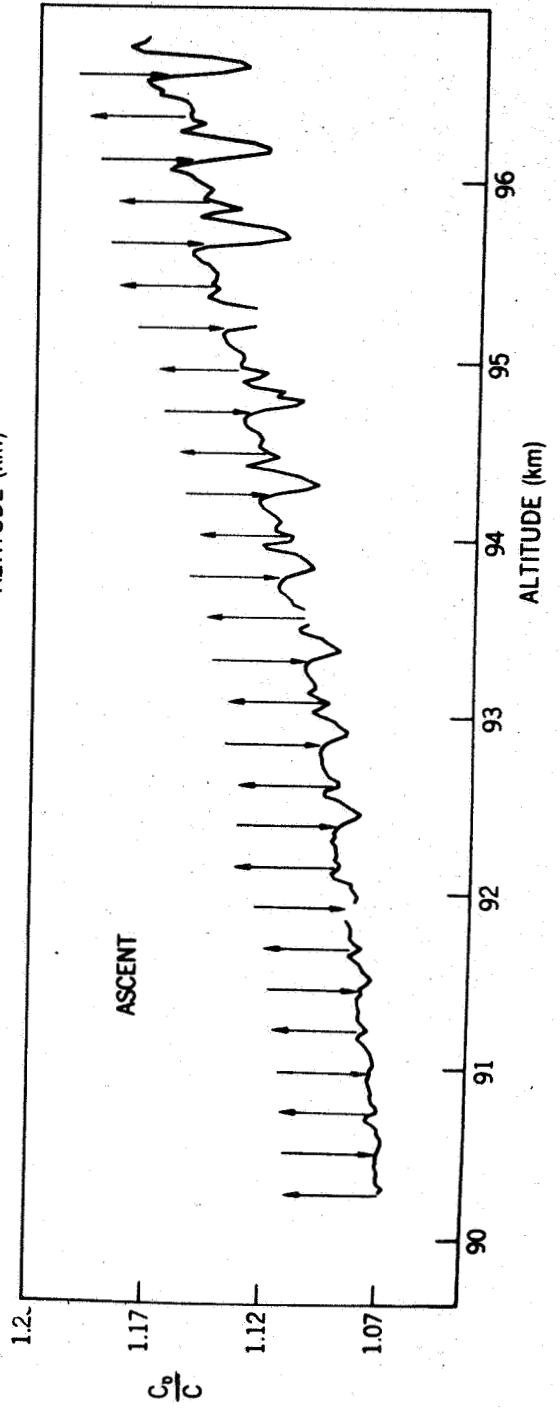
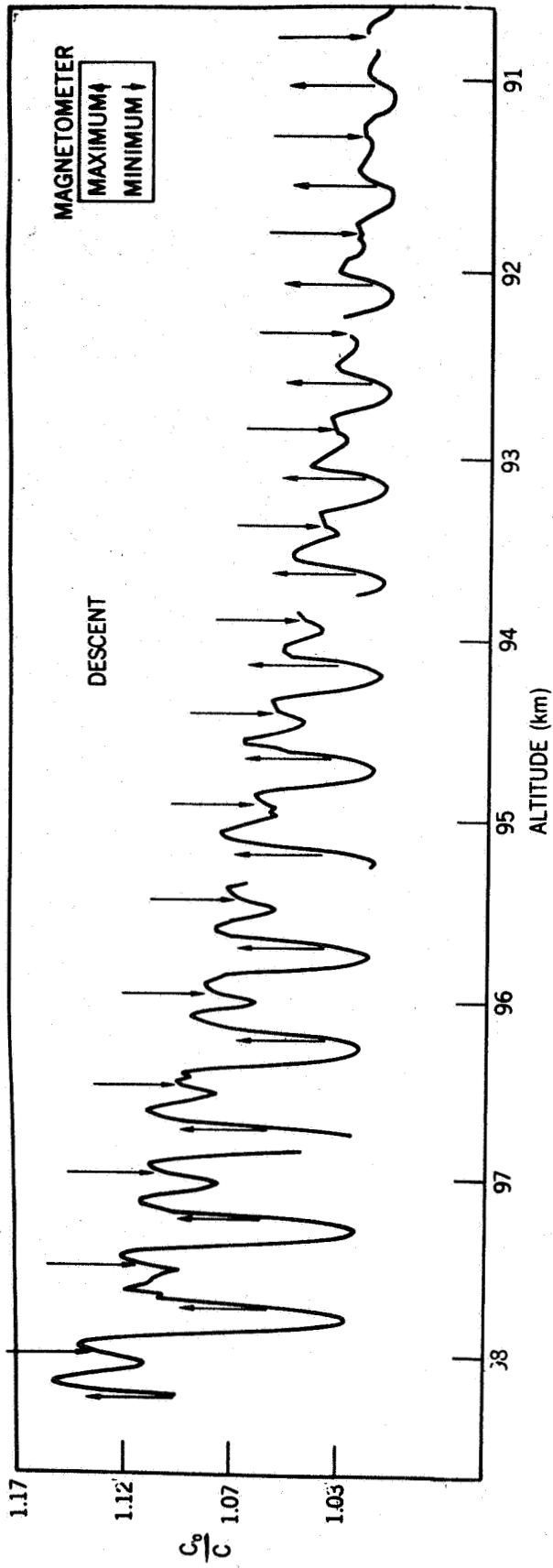
$\Delta f = 2 \text{ KHz}$

MONOPOLE EXPERIMENT

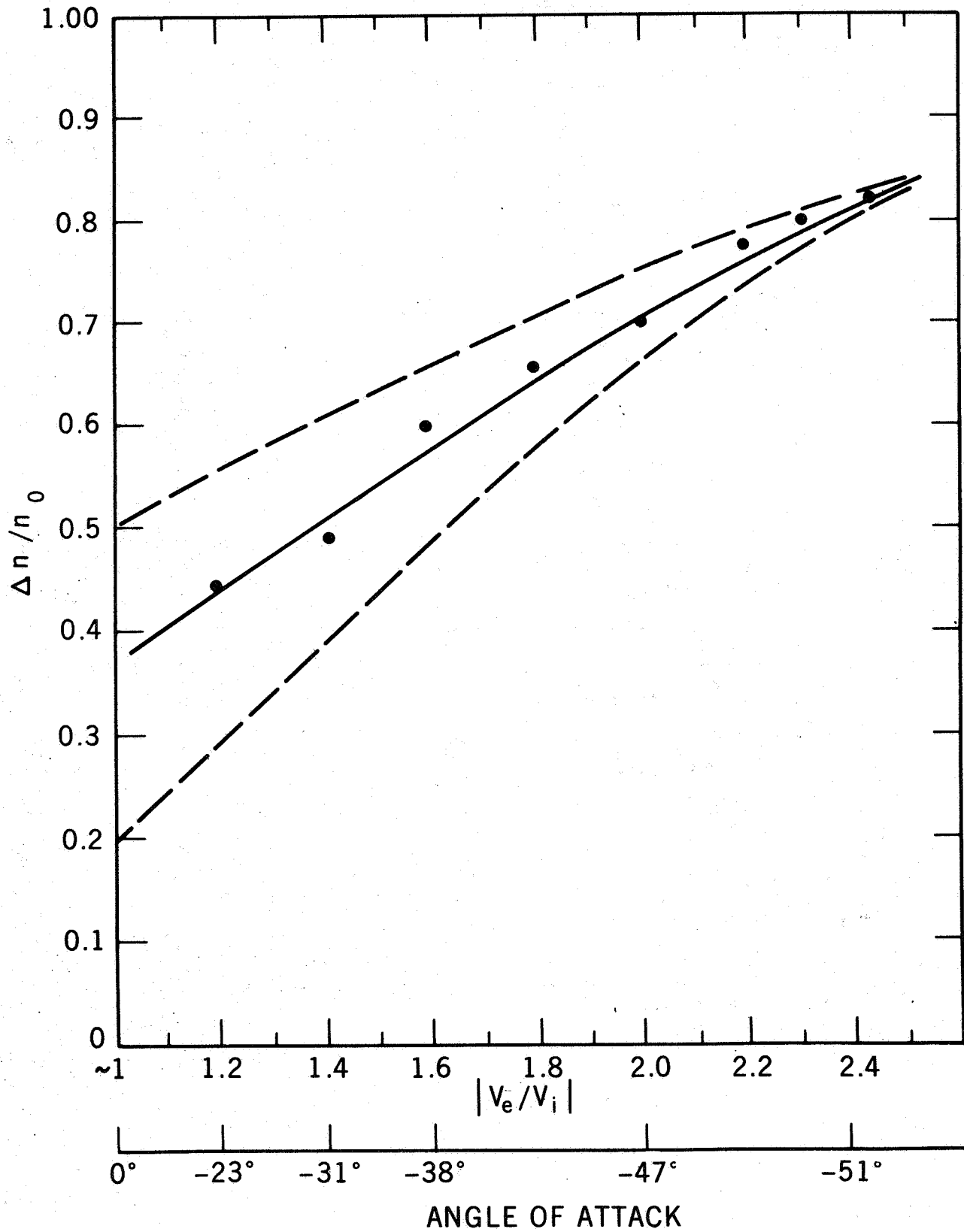
$f_0 = 4.44 \text{ MHz}$

$\Delta f = 15 \text{ KHz}$

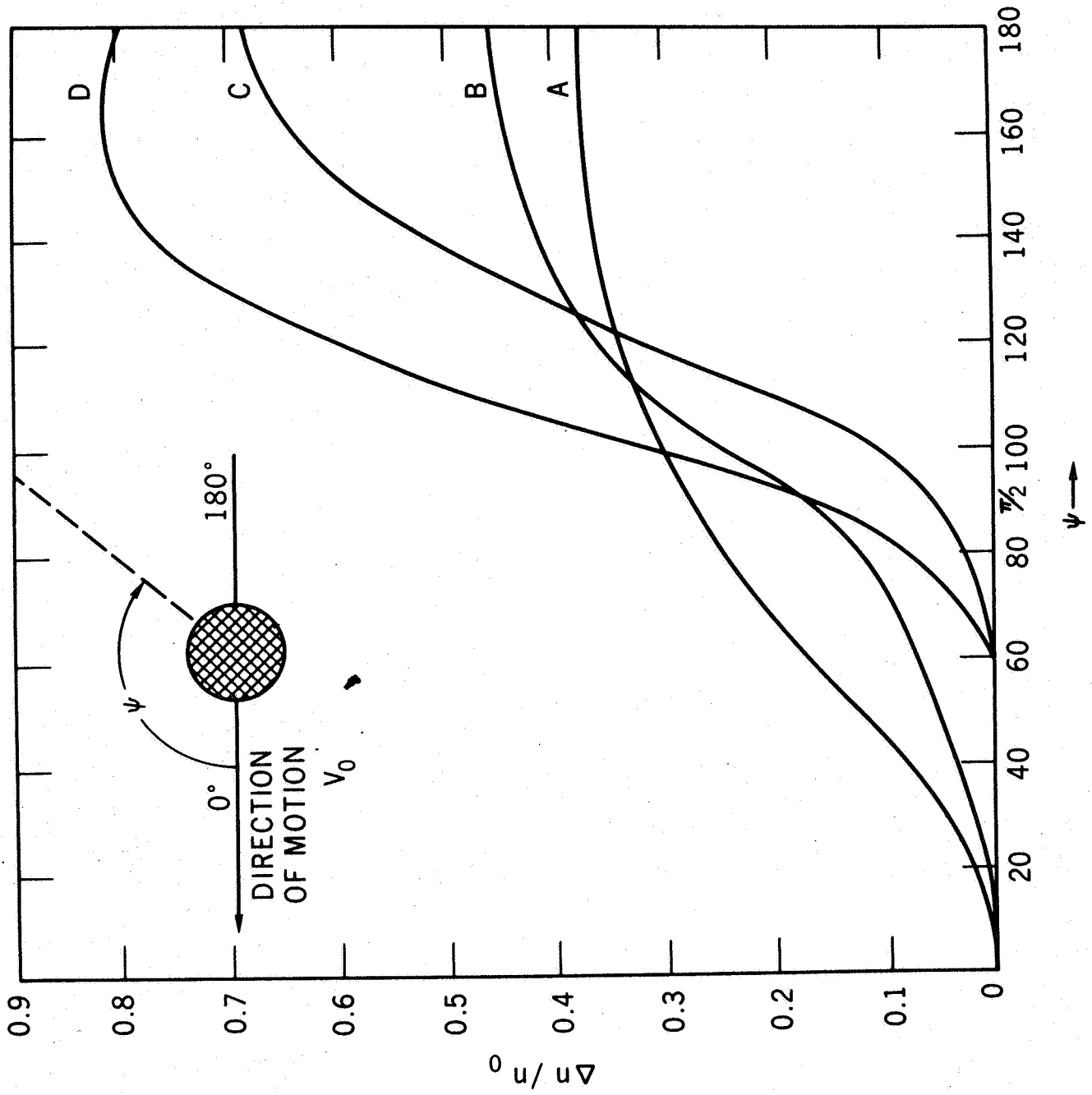




# FRACTIONAL WAKE ELECTRON DENSITY



# FRACTIONAL ELECTRON DENSITY VS. $\psi$



# FRACTIONAL ELECTRON DENSITY VS. $\psi$

